ELSEVIER

Geomorphology 38 (2001) 317–336

GEOMORPHOLOGY

www.elsevier.nl/locate/geomorph

Evolution of undercut slopes on abandoned incised meanders in the Eastern Highland Rim of Tennessee, USA

Hugh H. Mills [a,*], Richard T. Mills [b]

[a] *Department of Earth Sciences, Tennessee Technological University, Cookeville, TN 38505, USA*
[b] *Department of Computer Science, College of William and Mary, Williamsburg, VA 23187-8795, USA*

Received 23 May 2000; received in revised form 13 October 2000; accepted 8 November 2000

Abstract

Field surveys, location-for-time reasoning, and computer modeling were used to study the evolution of slopes on valley walls of abandoned bedrock meanders on the Eastern Highland Rim, Tennessee. Hillslopes on the undercut slopes of cutoff incised meanders were ordered as to relative age by the height of their meander floors above the modern stream level. The assumption is that the undercut slope is actively eroded by the stream until abandonment of the meander, at which time the slope begins to evolve to a different form. More-advanced stages of evolution occur on walls of higher meanders that were abandoned earlier. The most rapid change in this initial form is the elimination of a free face, which occurs soon after the meander is abandoned. In addition, the hillslopes associated with even the lowest (youngest) cutoff meanders show somewhat gentler overall gradients than the actively undercut slopes. Hillslopes associated with meanders 3 to about 20 m above modern stream level maintain straight segments with angles showing only a slight decrease from the 36–38° associated with the lowest cutoffs; overall angles decrease, however, as the straight segment becomes shorter. The oldest slopes, those on cutoffs 30 m or greater above modern stream level, have developed into convex–concave slopes with maximum slopes of 15°.

A hillslope evolution model based on previously published algorithms was used to simulate the transition of actively undercut hillslopes into hillslopes on abandoned meanders. Hillslope modeling is particularly useful in this setting. If the valley incision rate is known, an age can be estimated for the cutoff and hence for the hillslope. Alternatively, if hillslope process rates are known, a model age obtained for the hillslope can be used to estimate an incision rate. Even where both incision rates and hillslope process rates are poorly constrained, as in the present setting, modeling allows assumptions about specific rates to be evaluated by determining their implications for other rates. For example, for three cutoff meanders along one stream, best-fit criteria were used to select process rates for the model. Model ages of hillslopes were then obtained and compared with those calculated from a valley-incision rate measured elsewhere in the same physiographic province. For two of the hillslopes, model ages were found to be much younger than those calculated from the incision rate. In order to make the two ages agree, unreasonably low process rates had to be used in the model, thus implying that the incision rate probably underestimates the actual incision rate in this valley.

* Corresponding author. Fax: +1-931-372-3363.
E-mail addresses: hmills@tntech.edu (H.H. Mills), richard@stderr.org (R.T. Mills).

PII: S0169-555X(00)00104-5

Experimentation with heights of initial profiles, again using best-fit criteria, suggests that since abandonment of the highest cutoff, the plateau has been downwasting at a rate about one-fourth that of the valley incision rate, a finding in agreement with published rates of chemical denudation in the area.

Keywords: Hillslope evolution; Modeling; Cutoff meander; Incised meander; Eastern Highland Rim; Valley incision

1. Introduction

Evolution of hillslopes on resistant bedrock takes place so slowly that direct observation of change in most cases is impossible. One way to study this evolution is to order hillslope profiles according to their relative age and then to consider their forms to represent stages of a developmental sequence. In the unglaciated Appalachians and interior plateaus of southeastern North America, landscapes are poorly dated, and a chronosequence of hillslope profiles is difficult to find. One opportunity to do so is provided by incised meandering streams that show "ingrown" meanders (Rich, 1914) characterized by gentle slip-off slopes on the inside of the meanders and steep undercut slopes on the outside. Some of these meanders become abandoned when stream erosion cuts through their narrow necks. Once the meander is abandoned, the hillslope on the outside of the meander is no longer actively undercut and its profile evolves into a new form with gentler slopes. The higher the cutoff meander above the modern stream level (AML), the older the meander. The height AML of the meander allows hillslope age to be estimated from long-term stream incision rates. To study the development of these hillslopes over time, we wrote a process-response computer model utilizing the algorithms of Kirkby (1971, 1984, 1987, 1992). Our object was to infer process rates from profile form using best-fit criteria, to use these rates to estimate the ages of the profiles, and then to compare these ages with ages derived from stream-incision rates.

2. Previous work

The substitution of location for time is a long-established method of studying how landforms develop toward a characteristic form (Paine, 1985). A classic example of this method is that by Savigear (1952), who studied bluffs along the coast of Wales. After the post-glacial rise in sea level, a beach began growing eastward along the coast from Pendine, isolating the sea cliffs from the open sea. The slopes immediately east of Pendine, therefore, have been protected from undermining by waves for thousands of years, whereas slopes beyond the east end of the beach are still being attacked by waves. Thus, by inspecting a series of hillslope profiles from east to west, he could infer the sequence of hillslope development over time. Paine (1985) pointed out that the reliability of this technique depends highly upon how accurately the landforms can be ordered in time.

Carson and Kirkby (1972, pp. 318–319) pointed out an important limitation of the location-for-time approach. Although the method shows changes that occur over time, it does not necessarily reveal *how* they occur. For example, a decrease in hillslope angle might result from a decline in slope angle with time, but it could also result from slope retreat that replaces an existing gradient with a gentler one. Given this and other limitations, Carson and Kirkby (1972) suggested that the best approach to the study of hillslope development is through the study of hillslope processes and the construction of process-response models based on these processes. Process-response models can be combined with the location-for-time approach, as exemplified by Kirkby (1984) who applied a process-response model to the sequence of slopes studied by Savigear (1952).

Many modeling studies of hillslopes have been carried out. These studies have involved fault scarps (Nash, 1980, 1984; Colman and Watson, 1983; Hanks et al., 1984; Hanks and Wallace, 1985; Hanks and Schwarz, 1987; Mayer, 1984), marine or lake shoreline scarps (Colman and Watson, 1983; Kirkby, 1984; Hanks et al., 1984; Hanks and Wallace, 1985; Andrews and Bucknam, 1987; Rosenbloom and Anderson, 1994), fluvial terrace scarps (Colman and Watson, 1983; Nash, 1984; Pierce and Colman, 1986), and cinder cones (Hooper, 1995, 1998). Generally, the slopes have been underlain by unconsolidated

materials, although some have been underlain by bedrock (e.g., Kirkby, 1984; Rosenbloom and Anderson, 1994). One or more hillslope of known age was available for most of these studies. The age of hillslopes modeled has ranged from several thousand years to hundreds of thousands of years.

For the most part, modelers have used the diffusion equation approach of Culling (1960), commonly implemented with finite-difference or finite-element simulation programs, although analytical solution has also been employed. The diffusion equation $\partial z/\partial t = K\partial^2 z/\partial x^2$ states that the rate of change in elevation is proportional to local curvature of the slope. This approach assumes that mass-movement processes operative on the slope have transport rates that are directly proportional to slope and do not change as a function of x (distance downslope). Processes such as creep and rainsplash approximately fit this requirement; and as low scarps in unconsolidated material probably are degraded mainly by such processes, the diffusion equation generally provides a very good description of the change in scarp form over time. The diffusivity, K, is the "clock" of scarp erosion (Mayer, 1984) as it determines the rate of degradation in the diffusion model. When the age of a scarp is known, the scarp profile can then be used to estimate K. Subsequently, the K value can then be used to estimate the age of undated scarps in the same area from their scarp profile. The K values are often expressed as m^{3-1} ka^{-1}, or m^2 ka^{-1}, and reported values range from 1 to 16 m^2 ka^{-1} (Hanks et al., 1984). The value of K depends upon geologic and climatic conditions.

There are restrictions on the use of the diffusion model and some discrepancies in its application have been encountered. Among the restrictions, the diffusion model can be applied only after the hillslope reaches the angle of repose. A scarp in cohesive material may have a steeper slope, a "free face." The model does not apply during the interval of time required to reduce the free face to the angle of repose (Andrews and Hanks, 1985). In addition, the model applies only to the erosion of a transport-limited, not a weathering-limited, hillslope. Several authors have found that the scarp height has a greater than expected effect on diffusivity, indicating that the assumed linear relationship between slope and transport rate does not hold (e.g., Hanks et al., 1984; Mayer, 1984; Pierce and Colman, 1986; Andrews and Bucknam, 1987). At least two explanations are possible for this observation: (i) Other processes, such as wash, that are dependent upon downslope distance as well as on slope, contribute significantly to scarp degradation. Pierce and Colman (1986), for example, suggested that support for this interpretation was provided by the observation that K values in their study area were greater for poorly vegetated, south-facing scarps than for well-vegetated north-facing scarps. (ii) Transport processes are in fact functions of slope alone, but this function is nonlinear (Andrews and Bucknam, 1987). Pierce and Colman (1986), for example, suggested two mechanisms whereby creep rates might increase at greater than the first power of slope.

Most modelers have assumed a linear relationship between slope and transport. Several, however, have attempted to use a model that takes into account the nonlinear effects observed and/or to include erosional processes not modeled by linear diffusion. Andrews and Bucknam (1987), for example, modified the K parameter to $K(1 + 5s)$, where s is local slope. Hooper (1995) used a nonlinear diffusion equation. Rosenbloom and Anderson (1994) included in their model the bare bedrock weathering rate and a scaling depth for the rate at which weathering decreases with regolith thickness. The most encompassing modeling attempt, however, was that by Kirkby (1984), who included nonlinear as well as linear transport, degradation of the free face, and solutional erosion (details of this model are discussed in a later section).

The nomenclature of Wood (1942) and King (1953), in which hillslope profiles are divided into four segments, will be used herein. From top to bottom these are convex (waxing slope), cliff face (free face), straight (constant slope or debris slope), and concave (waning slope).

3. Physical setting

The Eastern Highland Rim of Tennessee is a plateau at an elevation of about 300 m situated between the Cumberland Plateau to the SE (elevation about 550 m) and the Central Basin to the NW (elevation about 200 m) (Fig. 1). The study area is

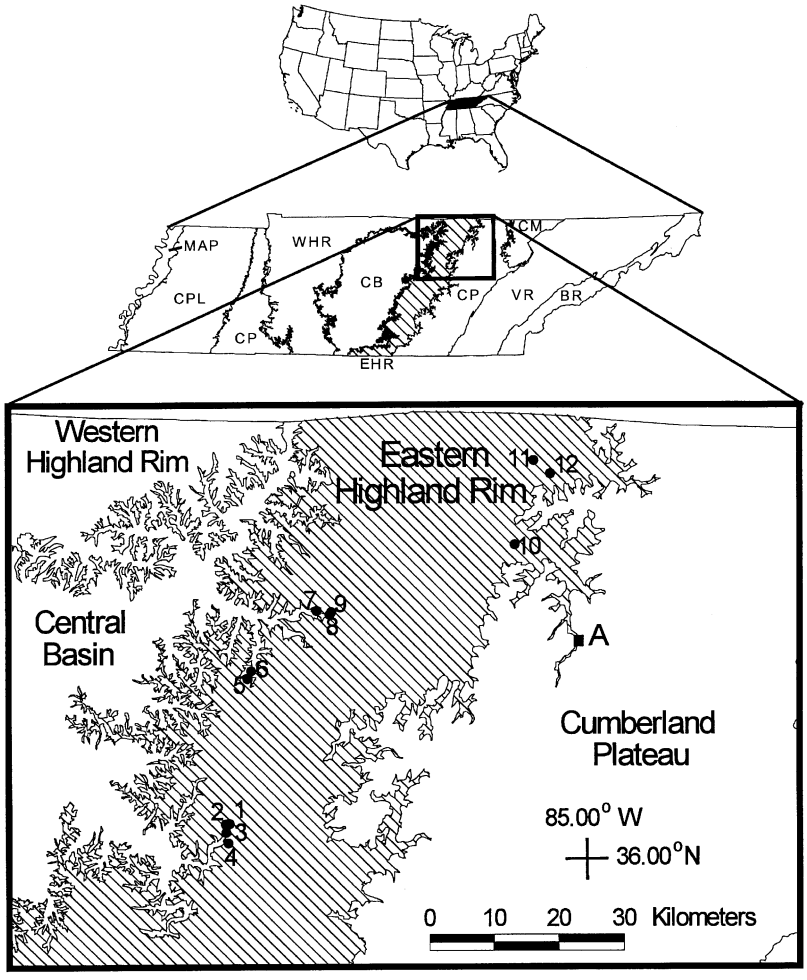

Fig. 1. Location map of study area. Numbers 1–12 show locations of studied abandoned meanders; A shows location of stream valley with incision rate determined by Sasowsky et al. (1995). Quadrangle and stream names are as follows: 1–3, Burgess Falls quadrangle, Cane Creek; 4, Burgess Falls quadrangle, Falling Water River; 5–6, Dodson Branch quadrangle, Blackburn Fork; 7–9, Windle quadrangle, Roaring River; 10, Riverton quadrangle, Obey River East Fork; 11–12, Moodyville quadrangle, Wolf River. Abbreviations for Tennessee physiographic provinces: MAP is Mississippi Alluvial Plain; CPL is Coastal Plain, loess-covered; CP is Coastal Plain; WHR is Western Highland Rim; CB is Central Basin; EHR is Eastern Highland Rim; CP is Cumberland Plateau; CM is Cumberland Mountains; VR is Valley and Ridge; BR is Blue Ridge.

underlain, for the most part, by five formations. From oldest to youngest these are the Leipers and Catheys Formations (Ordovician), commonly mapped as one unit; the Chattanooga Shale (Devonian and Mississippian); the Fort Payne Formation (Mississippian); and the Warsaw Formation (Mississippian). The Leipers–Catheys unit contains coarse-grained, fine-grained, and argillaceous limestone and has a maximum exposed thickness of 45 m. In the incised stream valleys, this unit crops out at the base of the slopes and on the valley floor. The Chattanooga Shale is a carbonaceous, fissile shale about 8 m thick and crops out in settings similar to the Leipers–Catheys. The Fort Payne Formation contains silicastone, calcareous siltstone, argillaceous limestone, and bands and nodules of dense chert. Much of its silica apparently formed by replacement of limestone. Fourteen samples from the Fort Payne in the Cane

Creek area (north of Burgess Falls in southern Putnam County) were dissolved in formic acid to determine the percent of insoluble materials by weight. This percentage ranged from 28.7 to 91.1, with a mean of 55.0. The Fort Payne thickness ranges from 50 to 75 m. Of the units described here, the Fort Payne is by far the most resistant to erosion and generally forms the steep valley walls along the incised streams. The Warsaw Formation is a limestone with various concentrations of sand, calcareous siltstone, calcareous shale, and argillaceous limestone. In the study area, this formation occurs mainly on the surface of the Highland Rim and its thickness ranges from 25 to 35 m (Wilson and Marcher, 1968). Regional dip is a fraction of 1° to the SE, but small local structures also occur.

The present mean annual temperature on the northern Eastern Highland Rim is about 15°C, and the mean annual rainfall is about 1320 mm. However, pollen records on the Rim demonstrate much colder temperatures during the last glacial maximum. For example, in a record from Anderson Pond (36°02′N, 85°30′W) at an elevation of about 300 m, Delcourt (1979) reported vegetation patterns for 18 ka that indicate mean annual temperatures near 0°C. Thus, periglacial conditions probably existed here during parts of the Pleistocene.

Many streams near the western margin of the Highland Rim plateau are deeply incised, flowing in gorges as much as 100 m deep. Generally, these incised valleys show ingrown meanders characterized by gentle slip-off slopes on the inside of the meanders and steep undercut slopes on the outside. Some of these bends have been abandoned when stream erosion cut through the narrow neck of the meanders (Figs. 2 and 3). The floors of these cutoff meanders range in height from 3 m to as much as 43 m above the modern stream. The age of abandonment thus varies greatly, and some idea of the antiquity of a cutoff can be gained by considering regional denudation rates and stream incision rates. Based on dissolved stream loads, Reesman and Godfrey (1981) found that the chemical denudation of the Central Basin is about 40 m Ma^{-1}. Since streams incised into the northwestern margin of the Highland Rim are graded to the Central Basin, a similar downcutting rate for these streams seems reasonable. Also germane to this question is the stream incision rate determined by Sasowsky et al. (1995) for the East Fork of the Obey River near the western edge of the Cumberland Plateau (site A in Fig. 1). Based on heights of palaeomagnetically dated cave passages above the present stream, they estimated this rate to be 60 m Ma^{-1}. Although the formations involved

Fig. 2. Oblique aerial photograph of large cutoff meander on Eastern Highland Rim (location 4 in Fig. 1). Width of meander floor is about 100 m.

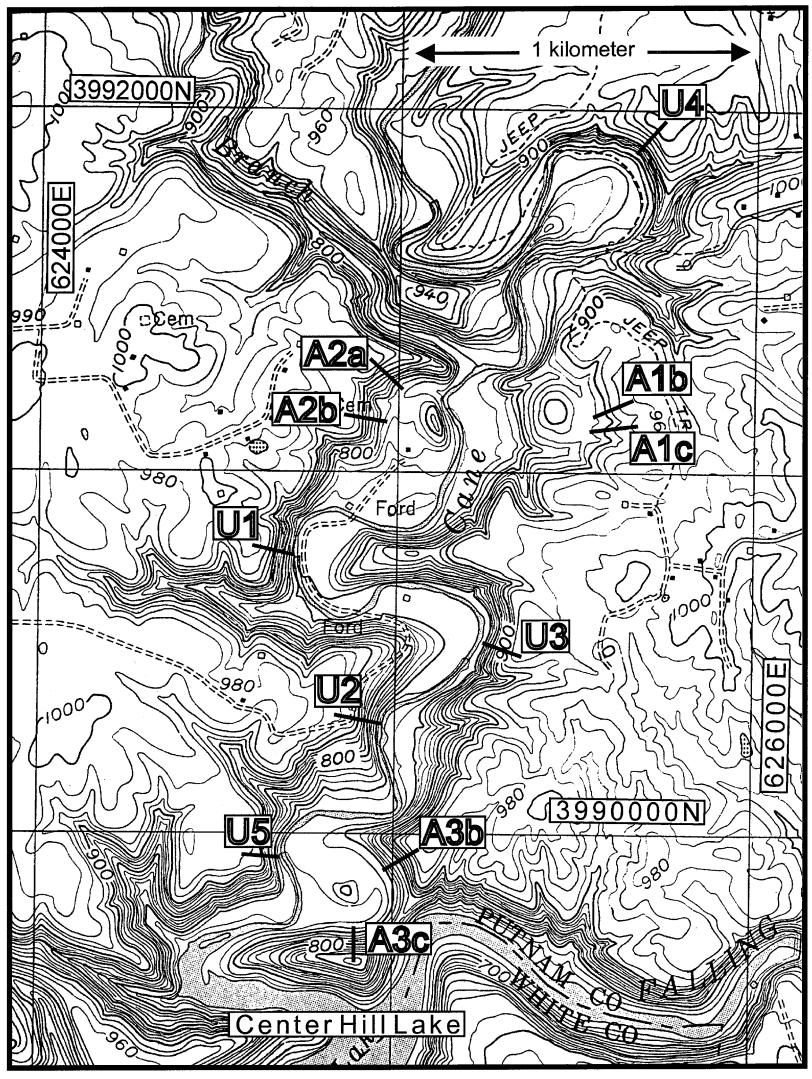

Fig. 3. Map showing area of concentrated study along Cane Creek. U indicates profiles on actively undercut slopes and A indicates profiles on undercut slopes of abandoned meanders. Meander A1 is 43 m above the modern stream level, meander A2 is 14 m above, and meander A3 is 3 m above. Grid squares are 1 km on a side. Eastings and northings are for UTM Zone 16.

are stratigraphically higher than those of the valleys considered here, the climatic and neotectonic settings of this river are similar to those of the incised Highland Rim streams, so this rate may be applicable. Taking the 40 and the 60 m Ma^{-1} as a probable range of incision rates, the highest cutoff meander was abandoned between 1.08 and 0.72 Ma. The incision rate may well have varied as a function of Quaternary climate change, although the 60 m Ma^{-1} rate was determined over a time span from 910 ka to the present (Sasowsky et al., 1995), and thus represents the incision rate averaged over a number of glaciations and interglaciations.

4. Methods

We selected for study twelve cutoff meanders together with nearby modern meanders, all with

similar stratigraphy. We used several approaches to describe the changes in the form of the undercut slope as a function of the height of the abandoned meander floor above the modern stream level. First, on topographic maps (scale 1:24,000, contour interval 20 ft [6.1 m]), we located the steepest slope on the outside of each meander. We then measured the angle of this slope over a vertical distance of 100 ft (30.5 m). These angles were then plotted against the maximum height AML of the abandoned meander floor. This height usually occurred about halfway around the meander loop, at a point farthest from the modern stream. (At the time of abandonment, of course, the floor was highest at the upstream end of the loop. Afterwards, however, dissection encroached from both ends of the loop, generally leaving the part of the loop farthest from the modern stream course at the highest elevation.)

Second, we surveyed 21 hillslope profiles on both active and abandoned undercut slopes by means of tape and clinometer. We examined the actively undercut slopes in order to determine the effect of stratigraphy on the form of slope profile and to estimate the probable original form of hillslopes on the abandoned meanders. In addition, we examined the form and steepness of the abandoned undercut slopes and related them to the height AML of the local meander floor.

Third, we made a detailed field study of the Cane Creek area (Figs. 1 and 3). This study included locating the stratigraphic contacts on each of the surveyed hillslopes, determining the whole-sediment particle size distribution at five representative sites, and running 11 seismic refraction lines (Mooney, 1984) in order to determine approximate thicknesses of colluvium on the floors and valley walls of abandoned meanders. Particle-size analysis was accomplished by sieve and hydrometer analysis, and supplemented by inspection at a large number of other points on the hillslopes, including "feeling" for silt and clay. We performed the seismic refraction using signals generated by a sledgehammer or a buried 8-gauge shotgun shell. Bedrock was identified by a seismic velocity of 3000 m s^{-1} or greater. For the seismic lines on the floors of abandoned meanders, we located lines along the centerline of the meander near the point at which the floor reaches its highest elevation AML.

Fourth, we wrote a computer model based on algorithms by Kirkby (1971, 1984, 1987, 1992) and Kirkby et al. (1992) in order to simulate the evolution of hillslope profiles. As did previous models by Kirkby, this model attempts to include multiple erosional processes. The disadvantage of such a model, as opposed to the simple linear diffusion models, is the large number of parameters for which values must be estimated. Despite this disadvantage, given the complexity of the hillslope evolution under consideration, we thought such a model to be the most realistic one. We then applied this model to hillslope profiles in the Cane Creek area.

The essentials of the model are as follows. The hillslope profile is divided into a series of equally spaced cells (51 in the simulations we ran), with the storage in each cell representing the elevation at a point on the hillslope. Between each time step, sediment fluxes into and out of each cell are calculated from empirical process laws for creep, wash, landslide, and solution; and from these the accompanying changes in the elevation of each cell are determined. Process rates depend largely upon the slope topography; i.e., distance from the divide and downslope gradient. A fixed time step of small enough size to prevent numerical instabilities is used.

"Creep" includes a group of processes which depend on gradient but not on collecting area and have no lower threshold. In the present setting, it consists mainly of soil creep and solifluction. Creep is assumed to carry sediment at a rate directly proportional to the downslope gradient. The sediment flux C out of a cell due to creep processes is given by:

$$C = Kg \tag{1}$$

where K is a constant giving the rate of creep and g is the downslope gradient ($\partial z/\partial x$).

"Wash" refers to overland flow able to entrain and carry soil particles on the surface. Unlike creep, wash depends on collecting area (i.e., distance from the divide) as well as on gradient. The general form of the process law for wash is:

$$W = kx^m g^n \tag{2}$$

where W is the sediment flux out of a cell due to wash processes, x is the distance from the divide, k

is a constant of proportionality, and m and n are exponential parameters. The values of m and n that are used vary greatly. For example, Pierce and Colman (1986) give a range of $m = 0.3–1.0$ and $n = 1.3–2$ for slope wash without gullying and $m = 1–2$ and $n = 1.3–2$ for slope wash with gullying. Determining the best values of m and n is considerably more difficult than determining other parameters in the model because m and n are exponents, so small changes in their values can result in large changes in the behavior of the hillslope model. Our data set has too many free parameters to be appropriate for estimating m and n, so we simply chose to use the values of $m = 2$ and $n = 1$ used by Kirkby et al. (1992), as this seems to give reasonable results. The specific form of the law is:

$$W = K(x/u)^2 g \tag{3}$$

where K is the creep constant, x is the distance from the divide, and u is the distance in meters beyond which the flux W due to wash becomes larger than the flux C due to creep. An advantage to the formulation of wash in this manner is that, whereas wash rates are generally unknown, u can be estimated to order of magnitude by field inspection. For example, a badland might have a value of 10 m; where wash is relatively insignificant, u might be greater than the hillslope length.

Landslides are modeled as a continuous process and hence the sediment flux due to landslides represents a long-term average rather than that due to individual events. The use of these average rates assumes that individual slides are small enough not to change the slope profile significantly. The flux due to landslides is controlled by four parameters, which are discussed in more detail by Kirkby (1984, 1987). Two of these parameters are thresholds: a lower, stable gradient g_ϕ below which there is no landslide activity; and an upper gradient g_t above which slides will never come to rest. The first threshold depends on the angle of internal friction and whether pore-water pressure can develop. Likely values of g_ϕ range from 0.14 (8°) for clays up to about 0.58 (30°) for some sandstones. The second threshold is usually related to the talus angle of repose, producing $g_t = 0.7$ (35°). The third parameter is a rate constant α that governs the rate of free degradation, or unconstrained lowering, D, which is given by:

$$D = \alpha g(g - g_\phi) \tag{4}$$

α may range from 0.001 m year^{-1} for sandstones to as much as 10 m year^{-1} for clays (Kirkby, 1987). The fourth parameter, h_0, indicates the average height from which blocks fall from cliffs, which should be roughly their mid-height. It is in a sense used to represent the momentum of the falling blocks in the expression for the mean horizontal distance h traveled by the moving material:

$$h = h_0/(g_t - g). \tag{5}$$

The value of h_0 influences how far a slide can run out across gently sloping ground at the base of a slope, but generally has only a slight effect on the slope profile elsewhere. Combining the expressions for detachment rate and travel distance, the sediment flux L_i out of cell i due to landslides is given by the discrete expression (Kirkby et al., 1992):

$$L_i = \frac{D\Delta x + L_{i-1}}{1 + (1/h)\Delta x} \tag{6}$$

where Δx is the spacing between cells, and L_{i-1} is the slide flux out of cell $i - 1$.

We chose to model solution as the rate of uniform, vertical lowering: during each iteration of the model, each cell is lowered by an amount determined by:

$$\Delta z_s = -r_s \Delta t \tag{7}$$

where Δz_s is the change in elevation of the cell due to solution, r_s is the rate of solution, and Δt is the time step. Unlike the other processes modeled, solution does not contribute to the flux of sediment being transported to cells downslope. Instead, any material eroded by solution is assumed to immediately leave the hillslope system.

For each iteration of the model, sediment fluxes out of each cell (and hence into the adjacent cell downslope) due to creep, wash, and landslides are calculated. These fluxes are then grouped into a total sediment outflux for each cell and converted into the resultant changes in elevation. The basis for this is the mass-balance, or continuity equation, which may be written as:

$$\frac{\partial z}{\partial t} = \frac{\partial S}{\partial x} \tag{8}$$

where $S = C + W + L$ is the total downslope flux of sediment, z is the elevation at distance x from the divide, and t is the elapsed time. Discretizing to allow numerical solution, this equation becomes:

$$\frac{\Delta z}{\Delta t} = \frac{S_{i-1} - S_i}{\Delta x} \tag{9}$$

where S_i is sediment flux out of cell i and S_{i-1} is flux out of cell $i-1$ and, hence, the flux into cell i. Once the rate of elevation change $\Delta z/\Delta t$ due to downslope sediment transport for a cell is calculated, the change in elevation is determined by multiplying by the time step Δt. Combining this rate of elevation change with that due to solution, the explicit expression for the elevation of a cell at time $t + \Delta t$ can be written:

$$z_{t+\Delta t} = z_t + \left(\frac{\Delta z}{\Delta t} - r_s\right)\Delta t \tag{10}$$

where z_t is the elevation of a cell at time t.

Due to the inherent limitations of computer models, a few somewhat artificial assumptions must be made. At the divide, the calculated downslope sediment flux is doubled because an equal amount of sediment is assumed to leave in each direction (the rate of solution is *not* doubled). At the final basal cell, provision is made for the user to choose whether all sediment delivered from upslope is to be removed or whether a fixed percentage of entering material is to be retained. In the interest of numerical stability, negative elevations are not allowed; if a cell's calculated elevation comes out negative, it is set to 0. Generally, solution is the only process that would cause negative elevations were this requirement not imposed.

Note that if only the creep term of the total sediment flux S is used, our model can be reduced to the simple linear diffusion equation. Considering creep processes only, we have $S = Kg$. Substituting this expression into the mass balance (Eq. (8)), we get:

$$\frac{\partial z}{\partial t} = K\frac{\partial}{\partial x}g. \tag{11}$$

But the gradient $g = (\partial z/\partial x)$, so Eq. (11) becomes:

$$\frac{\partial z}{\partial t} = K\frac{\partial}{\partial x}\left(\frac{\partial z}{\partial x}\right) = K\frac{\partial^2 z}{\partial x^2} \tag{12}$$

which is the simple linear diffusion equation.

The model was applied by estimating the form of the initial profile from nearby actively undercut slopes, and then running the model until this profile had "evolved" into a form approaching that of a particular profile on an abandoned meander. The program computes the mean absolute difference between the initial profile and the "target" profile after each iteration and records the minimum mean absolute difference for each run—i.e., the "best fit." (The minimum mean squared difference was also computed, although we preferred to use the minimum mean absolute difference as a measure of best fit, owing to the lesser effect of large localized differences between profiles. In fact, however, the two methods almost always gave very similar results.) As an aid to finding the best fit, our program allowed the position of the initial profile to be moved various distances to the left or right of the target profile. The program is written in Visual Basic. Executables, source code, and documentation are all available at http://stderr.org/~hds or may be requested from the authors.

Unlike many modeling studies, we had no dated hillslopes. Further, the incision rates are only estimates, and process rates are unknown. Nevertheless, we hope to show that modeling can increase our knowledge by testing the consequences of certain assumptions. For example, different combinations of rate constants, obtained from ranges reported by previous researchers, were tested to see which combination gave the best fitting profile. The resulting model age was then compared with the hillslope "age" estimated from the height AML of the cutoff meander using the incision rates of 40–60 m Ma^{-1}. Alternatively, rate constants were adjusted so as to make the model age equal to the age estimated from incision rates, and the fit was evaluated.

The target slopes are simply the surveyed profiles of the outside slopes on the cutoff meanders. The initial slopes, however, although based on profiles of presently undercut slopes, must be modified from the latter because the depth of the gorge was probably lower when the cutoff meanders were abandoned than it is now, so that the initial hillslope height was probably less than that of presently undercut slopes. Thus, the profile of the latter cannot be used in its present form but must be modified so as to approximate the undercut slopes as they were at the time of

meander abandonment. This modification contains two steps. First, the height of the hillslope at the time of abandonment must be estimated. This was done based on the following rationale involving the relative rates of valley incision and plateau lowering. The two extreme possibilities are that (i) the plateau has not lowered at all, and (ii) both have been lowering at the same rate (the "dynamic equilibrium" hypothesis). Consider, for example, a valley 90 m deep with a cutoff meander whose floor is 30 m above the valley bottom. Under the first assumption, the hillslope on the outside of the cutoff meander was 60 m high at the time of abandonment, the same as today. Under the second assumption, the hillslope was 90 m high, the same as actively undercut hillslopes in the valley today.

More likely than either of these extremes, the plateau surface has been lowering but at a rate less than that of the valley incision. For example, if the plateau has been lowering at half the rate of the valley, the original height of the cutoff meander hillslope would be $(0.5 \times 30) + 60$, or 75 m. We dealt with this uncertainty as follows. We considered the possibility that the plateau lowered at a rate 0%, 25%, 50%, 75%, and 100% that of the valley (i.e., 0% means that the plateau does not lower at all, 50% means that the plateau lowers half as rapidly as the stream incises, and 100% means that the plateau lowers at the same rate as the stream incises). For each case, we calculated the height of the initial slope and then modeled the evolution of that profile to the same target profile. For each hypothesized ratio, we ran the model 17 times using various combinations of rate constants. We then ascertained which ratio produced the best fits and used this evidence to infer the most-probable ratio. The most-probable ratio then allowed the height of the initial hillslope profile to be estimated.

Except for the 100% case, initial profiles will be lower than the 90-m heights of presently undercut slopes. The second step, then, is to lower the profiles of modern slopes to the heights indicated by the results of step one. The simplest approach would be to compress the profile proportionately. For example, if the original slope height is estimated to be 60 m and that of the actively undercut slope is 90 m, the profile of the latter slope could simply be compressed so that it maintains its original form but is only two-thirds of its original height. However, our inspection of undercut slopes in Eastern Highland Rim valleys that have been incised to different depths suggests that this procedure would be erroneous. Instead, the lower, steeper parts of the profiles appear relatively constant regardless of gorge depth, but the upper slopes are steeper where valleys are deeper. Therefore, modification of the modern profiles was accomplished as follows. The lower, steeper part of the profile (roughly the lower one third) was retained at its actual scale, whereas the upper part of the profile was compressed proportionately to achieve the desired profile height.

One additional reason for modifying the profiles of actively undercut slopes is that the plateau surface is not a plane but a gently rolling surface, so that the height of actively undercut slopes varies from place to place. Because of such fluctuation, for the 100% case sometimes the "initial" profile was found to be slightly lower than the target profile of the nearby abandoned meander, requiring adjustment of the profile prior to modeling.

5. Results and discussion

Fig. 4 shows the relationship between the height of the cutoff meander floor above the present stream and the steepest slope angle (as measured over a height of 100 ft [30.5 m] on topographic maps). Note that the maximum slope angles associated with even the lowest (and therefore youngest) of the abandoned meanders are 10–15° lower than those of the actively undercut hillslopes; the initial rate of relaxation after abandonment is thus very rapid. This decline probably reflects the rapid disappearance of the free face. If only the abandoned meanders are considered, the height of the cutoff meander explains 76.7% of the variance of the steepest slope angle ($p < 0.01$).

The average slope angle is a crude measure of slope character, and surveyed slope profiles reveal much more about the process of slope evolution. Cane Creek, north of Burgess Falls in southern Putnam County, TN (Figs. 1 and 3), was the location of the most intense field study, and discussion is confined mainly to this location. Here, three cutoff meanders, ranging in height above the modern stream from 3 to 43 m, occur in close proximity to one

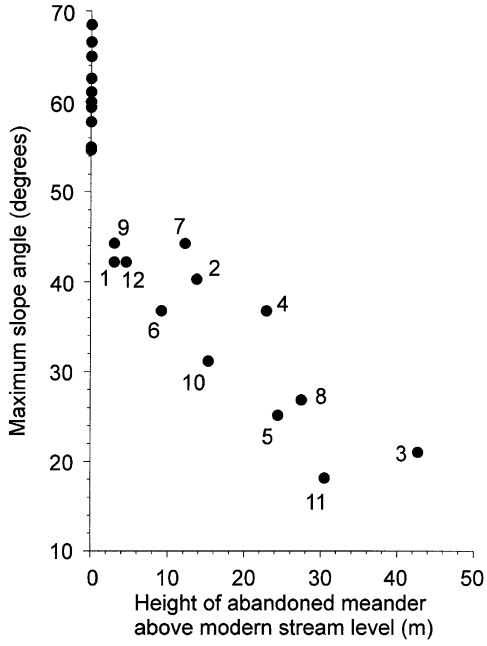

Fig. 4. Maximum slope angle (measured over 100 ft [30.5 m] vertical distance on topographic map) as a function of height of the abandoned meander above the modern stream. Numbers refer to site locations in Fig. 1. Unnumbered points on the *y*-axis are actively undercut slopes located near the abandoned meanders.

another (Fig. 3). To visualize the form of these slopes at the time of abandonment, Fig. 5 shows profiles of five actively undercut slopes on the outsides of ingrown meanders still occupied by streams. Profile U4 is the farthest upstream and occurs upstream from the point at which the stream has incised through the resistant Fort Payne Formation into the weaker formations beneath, and as a consequence differs greatly from the other profiles. It shows a near-vertical cliff about 15 m high surmounted by a long convex slope that has a gentler angle than the other profiles. The remaining four profiles have the weaker formations cropping out at their bases and display their steepest slopes above the Fort Payne/Chattanooga contact. They are roughly similar, except that U5 has a dramatically steeper slope in the Fort Payne; the slope overhangs for a vertical distance of more than 30 m. Bedding appears to be no thicker here than elsewhere, and why the slope is so much steeper is not apparent. By comparison with the ideal slope profile of Wood (1942), all profiles display the upper two segments. However, the straight segments are not well developed because of the presence of ledges, and the lower concavity is almost absent, as might be expected for slopes being actively eroded by streams.

Fig. 6 shows profiles on undercut slopes of abandoned meanders. Note that the slopes are formed almost completely on the Fort Payne Formation. At two of the three meanders, abandonment appears to have occurred soon after the stream incised through the Fort Payne into the weaker units beneath; this association may reflect greater rates of lateral migration by the stream below this contact. The top of each profile is close to the surface of the plateau (altitude about 290 m). The meander floor at A3 is about 3 m above the modern stream, at A2 is 14 m above, and at A1 is 43 m above. The differences in the vertical extent of the profiles reflect in part the

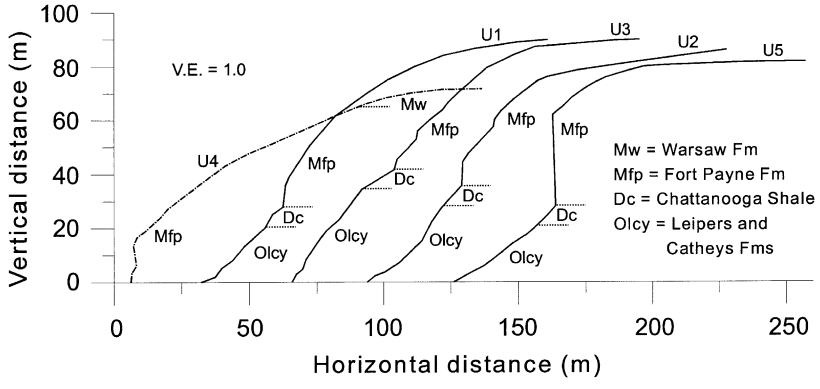

Fig. 5. Profiles on actively undercut slopes at Cane Creek, showing geological contacts. Locations of profiles are shown in Fig. 3.

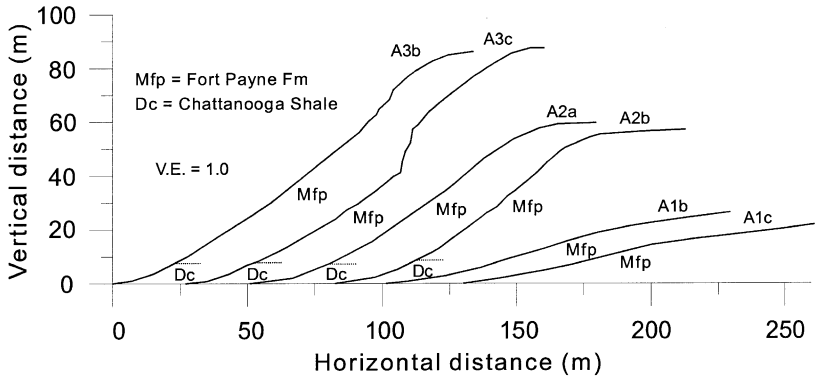

Fig. 6. Profiles on abandoned undercut slopes at Cane Creek, showing geological contacts. Locations of profiles are shown in Fig. 3.

height of their associated abandoned meander above the modern stream. The A1 profiles are much lower than the A2 profiles because the cutoff meander at A1 is much higher above the modern stream. The A3 profiles have a particularly large vertical extent not only because the A3 cutoff is near the modern stream level, but also because it occurs farther downstream than A1 and A2 where the stream has incised more deeply below the plateau surface than it has upstream.

The differences in the forms of the profiles at A1, A2, and A3, however, presumably reflect mainly the difference in the amount of time that has transpired since the undercut slopes were abandoned. All of the profiles have an upper convexity, but only A3c still clearly has a cliff face; A3b has merely the suggestion of a cliff face. The difference between these two profiles apparently reflects a very thick, massive bed of silicified limestone that occurs only at A3b. The four younger profiles (A3a, A3b, A2a, and A2b) all have straight segments and lower concavities. The oldest profiles, A1b and A1c, have developed into convex–concave slopes with only a suggestion of a straight segment between. The angles for the straight segments are 36° and 38° for A3, 34° and 35° for A2, and 14° and 16° for A1. There is thus little difference between the straight segments at A3 and A2. The 34–38° range is typical of talus slopes; however, as shown in Table 1, there seems to be too much silt and clay in the debris for it to behave as talus. Talus can stand at an angle close to its angle of internal friction (ϕ) because its interstices are too large to allow significant pore-water pressure to develop even during intense rainfall. However, the amount of fine material in the debris mantles of A3 and A2 should be sufficient to impede drainage and allow complete saturation, which would produce a maximum slope angle θ such that, approximately, $\tan\theta = 1/2 \tan\phi$ (Skempton, 1964), which, for the ϕ values shown in Table 1, would be only 21–25°. In fact, however, the observed maximum angles are much closer to the drained ϕ values than they are to these lower angles. This finding is difficult to explain, except by assuming that slope is at least partly controlled by factors

Table 1
Particle-size analysis and estimated angle of internal friction

Slope profile	% Gravel	% Sand	% Silt	% Clay	Estimated ϕ (°)[a]
A1b	50	12	31	7	38
A2a	56	17	26	1	38
A2b	62	9	23	6	42
A3b	67	10	18	5	43
A3c	53	10	31	6	38

[a]The ϕ values were estimated from the triangular diagram in Kirkby (1973, his Fig. 5) relating ϕ to particle-size distribution.

other than the mechanics of the surficial mantle. One possible explanation is that bedrock ledges act to "dam" debris and thereby increase the slope from what it would be if the hillslope lacked ledges.

Although the overall slope angles are steeper for the A3 slopes than for the A2 slopes, the mean slope difference between the two is only 2.5°—there is essentially no difference. The decrease in overall slope angle from the A3 to the A2 slopes appears to have been achieved by retreat of the cliff face. The A1 profiles differ greatly from the A3 and A2 profiles, the angles of the latter being less than half as great. These differences are difficult to explain by means of differences in the mantle, however, for as Table 1 shows, the particle-size distributions display little variation. Again, it appears that factors other than mantle characteristics are affecting profile development.

Hillslope profiles surveyed along other streams generally appear similar to those at Cane Creek, indicating that the studies at Cane Creek are applicable to locations elsewhere on the Highland Rim.

The thickness of colluvium must be considered in interpreting the results of this study. In the first place, once a meander loop is abandoned, colluvium from the valley walls may encroach onto and cover the valley floor. If the thickness of this colluvium is substantial, the height of the meander above the modern stream may be inflated. Froelich et al. (1992), for example, drilling in the floors of abandoned incised meanders in the Valley and Ridge of West Virginia and Virginia, found colluvium fills as thick as 19 m, with an average exceeding 8 m. This finding suggested that colluvium on meander floors could indeed be a problem for estimating the true height at which meander abandonment occurred. Therefore, an effort was made to determine the thickness of fill in several cutoff meanders at Cane Creek by means of seismic refraction. The depth to bedrock for the cutoff meander floors ranged from 2.4 to 4.0 m (Table 2). For comparison, on two low stream terraces located away from valley walls, the depth to bedrock, presumably mainly in alluvium, was 3.6 and 4.4 m. These results are compatible with observations on present-day streams, which flow mainly on bedrock and generally reveal no more than 2–3 m of alluvium below the surface of the flood plain. Hence, although significant colluvial deposits may occur on the hillslopes themselves, the centerlines of the cutoff meanders appear to have undergone little colluviation.

Table 2
Depth to bedrock as determined by seismic refraction on floors of abandoned meanders

	Line 1 (m)	Line 2 (m)
A1 meander floor	4.0	–
A2 meander floor	2.4	3.6
A3 meander floor	3.2	3.4
Low terrace of present stream	3.6	4.4

It is also desirable to know the colluvium thickness on the lower ends of the hillslopes associated with the abandoned meanders. Seismic lines were run along slope on four profiles. However, signals proved to be severely attenuated in this loose material, and only *minimum* thicknesses could be obtained. These thicknesses were >7.9 and >9.4 m at A3, >8.8 m at A2, and >9.7 m at A1. These values establish the presence of thick colluvium on the lower slopes, demonstrating that they are at least substantially depositional, and provide a quantitative measure in addition to profile form to use for testing models.

The hillslope evolution model was applied to one profile from each of the Cane Creek cutoff meanders (A3b, A2a, and A1b in Fig. 3). The first problem was to determine the height of the initial slopes, as discussed in the Methods section. Fig. 7 shows examples of manufactured initial profiles for the various hypothesized ratios between plateau lowering rate and valley incision rate. Table 3 shows the combination of process rates used in the 17 computer runs for each case. For A1b, the 43-m-high cutoff, the assumption that the plateau was lowering at 25% of the valley incision rate gave the best fit 12 out of 17 times, 0% gave the best result 4 times, and 100%, 1 time. Hence, it appears that the 25% hypothesis is strongly supported by the best-fit criteria. This finding is in agreement with chemical denudation rates reported by Reesman and Godfrey (1981), who reported rates of 40 m Ma^{-1} for the Central Basin (to which Cane Creek is graded) and 11 m for the Highland Rim (which forms the plateau above Cane Creek).

The two lower hillslopes, however, showed different results. Profile A2a, associated with the 14-

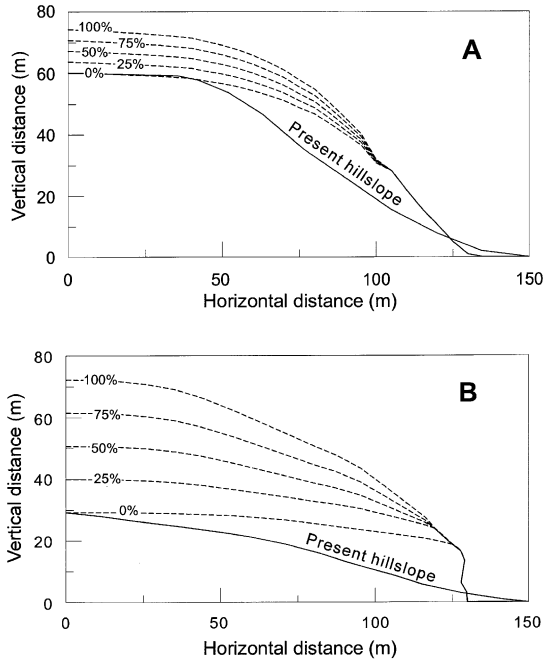

Fig. 7. Initial profiles used for modeling assuming rate of plateau lowering is 0%, 25%, 50%, 75%, and 100% that of valley incision rate. (A) Initial profiles used for modeling intermediate cutoff (profile A2a). (B) Initial profiles used for modeling highest cutoff (profile A1b). Explanation of the procedures used in deriving the initial profiles is in text.

m-high cutoff, showed best fits for the 0% case 11 times, for the 25% case 4 times, and 50%, 2 times. Profile A1b, associated with the 3-m-high cutoff, showed less consistent results, as might be expected where the height difference between the 0% and 100% profiles is only 3 m. Nevertheless, A1b showed best fits for the 0% case 8 times vs. 4 times for the 25% case and 2 times for each of the remaining three cases.

Such a discrepancy between the profile on the highest cutoff and those on the lower ones may be reasonable. The 43-m-high cutoff is located well up in the Fort Payne Formation so that much of the post-abandonment valley incision has been into that resistant formation. However, the two lower cutoffs have their floors below the Fort Payne in the much less resistant Chattanooga Shale and Leipers–Catheys Formations. Hence, the valley incision rates subsequent to the abandonment of these meanders may have been very rapid, during which time the Fort Payne-capped plateau surface has lowered very little. Thus, for the slopes associated with these two cutoffs, the zero-lowering case may be essentially true. Hence, for initial profiles used in the modeling, the 25% case was assumed for the highest cutoff and the 0% case for the two lower ones.

Once the initial profiles had been selected in this manner, the next step was to explore the effect of varying process rates on model fit and model age. Of the parameters in the model, some have greater effects either because the range of plausible values is greater or because model age is very sensitive to the value used. Preliminary consideration or modeling showed that three of the model parameters are relatively less important. The talus angle, g_t, was assumed to be 35° and is not likely to vary much. The landslide travel distance, h_0, was found to have some effect on fit but little effect on model age. A value of 60 m, about half the slope length, was assigned for this parameter. The landslide threshold angle, g_ϕ, was assigned a value of 23°. Smaller values as low as 15° did not have a great effect on model results.

The remaining four parameters were much more important for model results. To explore the effects of these, we first selected likely values for each. For creep rate, K, we used 3 m^2 ka^{-1}, a value intermediate between that of normal creep and solifluction, since the hillslopes have probably been exposed to periglacial or near-periglacial conditions during part of their existence. For the distance at which wash becomes more important than creep, u, we reasoned that since there was little evidence of wash on the slopes we would use a value roughly equal to the length of the slope, 120 m. For solution rate, we used 10 mm ka^{-1}, approximately the erosion rate on the Highland Rim surface measured by Reesman and Godfrey (1981). The rate of free degradation above threshold, α, is the most poorly constrained rate. Young (1972, p. 123) provided an estimate of cliff recession on hard rock under humid temperate climatic conditions of 1 mm $year^{-1}$. Given the highly resistant nature of the Fort Payne Formation, we used this value as an initial estimate.

We next determined the sensitivity of model fit and age to values of the four above parameters as follows. Using the values specified above, we kept the values of three of the parameters constant while

Table 3
Initial profiles providing the best-fitting model profiles for 17 sets of transport-rate values[a]

Creep rate (m^2 ka^{-1})	Wash > creep (m)	Solution rate (mm ka^{-1})	Rate of free degradation above threshold (mm $year^{-1}$)	Initial profile with best fit to A1b profile (%)	Initial profile with best fit to A2b profile (%)	Initial profile with best fit to A3b profile (%)
1	120	10	1	0	0	0
10	120	10	1	25	0	0
30	120	10	1	25	0	0
100	120	10	1	25	25	75
300	120	10	1	25	50	100
30	10	10	1	0	0	25
30	30	10	1	0	0	25
30	60	10	1	0	0	0
30	240	10	1	100	0	0
30	120	1	1	25	0	0
30	120	30	1	25	0	25
30	120	50	1	25	25	50
30	120	100	1	25	25	75
30	120	10	0.1	25	50	100
30	120	10	0.5	25	25	50
30	120	10	3	25	0	0
30	120	10	10	25	0	0

[a]The four columns on the left show the sets of process rates used for the modeling. The three columns on the right show which of the initial profiles allowed the best fit to each of the three target profiles. "0%" refers to the initial profile based on an assumption of no plateau lowering, "25%" refers to that based on an assumption that the rate of plateau lowering was 25% that of the rate of stream incision, etc.

varying the fourth. At least eight values were used, and the fit (i.e., the minimum mean absolute difference) and the model age were recorded for each run. This was done for each of the three modeled profiles (Fig. 8).

The results of this sensitivity analysis allow several inferences to be drawn. First, note that for the two younger profiles, model age is affected mainly by rate of free degradation above threshold (α), and that the effects of other rates are minor if extreme values are neglected (e.g., a value of 10 m for u is likely to be found only in badlands). In contrast, for the oldest profile, α has little effect on age, whereas the values of the other three parameters are much more important.

Second, note that regardless of the values of parameters used, profile A3b (associated with a cutoff only 3 m AML) is shown to be older than profile A2a (associated with a cutoff 14 m AML). This result will be discussed further below.

Third, we used the information on fit provided by Fig. 8, together with other considerations, to estimate the most appropriate values of parameters to use for further modeling. For creep rate, the best-fit value for A3b is 5 m^2 ka^{-1} and that for A2a is 3 m^2 ka^{-1}. All that can be said for A1b is that the rate is above 1 m^2 ka^{-1}. Based on the values from A3b and A2a, however, plus the likelihood of a value intermediate between 1 and 10 m^2 ka^{-1}, we chose a value of 4 m^2 ka^{-1}. For the distance at which wash becomes greater than creep, the best-fit value for A3b is 50 m, for A2a is 100 m, and for A1b is 150 m. Hence, we chose a value of 100 m. For solution rates, the best-fit value for A3b is 40 mm ka^{-1}, for A2a is 10 mm ka^{-1}, and for A1b is 40 mm ka^{-1}. We therefore chose a value of 30 mm ka^{-1}. For the rate of free degradation above threshold, the best-fit values for both A3b and A2a are 0.8 mm $year^{-1}$. For A1b, all that can be said is that the lower the value, the better. Given, however, that the fit and age of A1b is

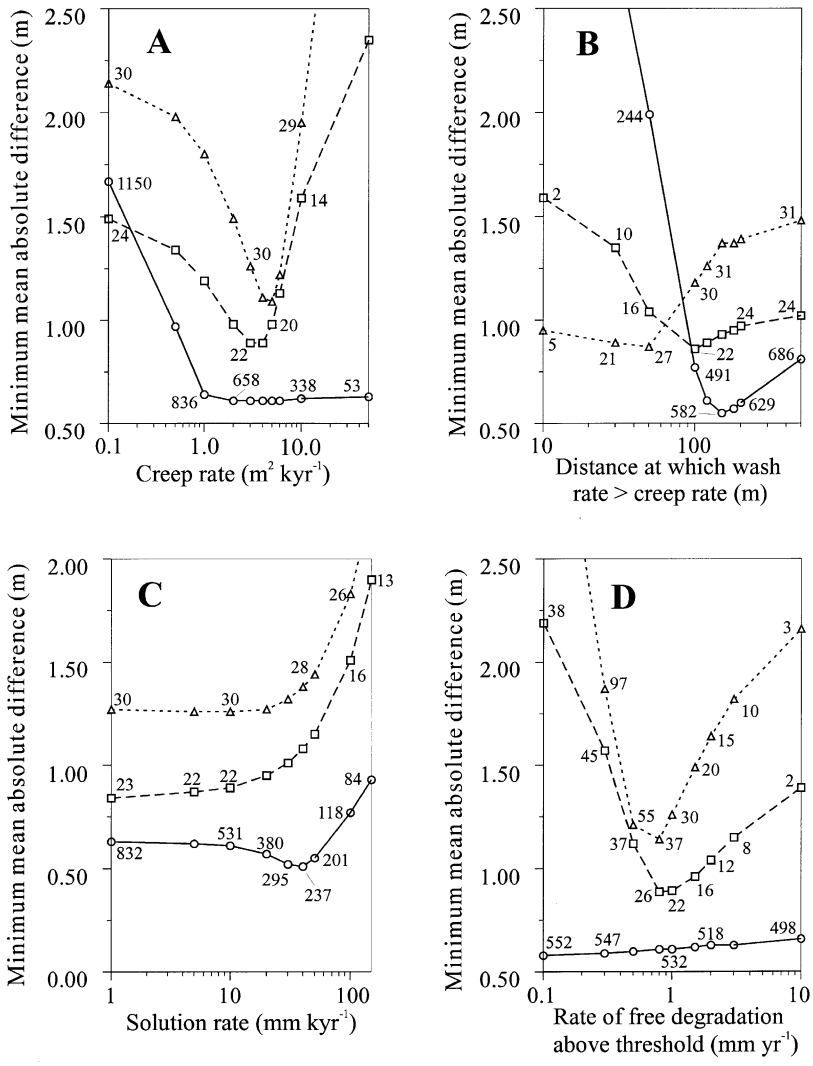

Fig. 8. Sensitivity analysis for modeling of three Cane Creek profiles. Both fit (i.e., minimum mean absolute difference between actual profile and model profile) and model age are shown as a function of varying process rates. Profile A1b (highest cutoff meander) results are shown by solid line, profile A2a (intermediate cutoff meander) by long-dash line, profile A3b (lowest cutoff meander) by short-dash line. Numbers show model ages in thousands of years. (A) Creep/solifluction rate (K). (B) Distance at which wash becomes greater than creep (u). (C) Solution rate (mm ka^{-1}). (D) Rate of free degradation above threshold (mm year^{-1}).

insensitive to this value, plus the fact that 0.8 is close to Young's (1972) estimate of 1.0 mm year^{-1}, we selected 0.8 mm year^{-1} as the most appropriate value.

We then used the above parameter values to model all three profiles, and good fits to the target profiles resulted (Fig. 9). Slightly better fits can be obtained by using different parameter values for each profile, but we think that fits obtained using the same parameter values for all three profiles have greater validity. Note that the model ages of two of the hillslope profiles differ somewhat from those predicted from the estimated incision rates. If we assume the 60 m Ma^{-1} incision rate discussed previ-

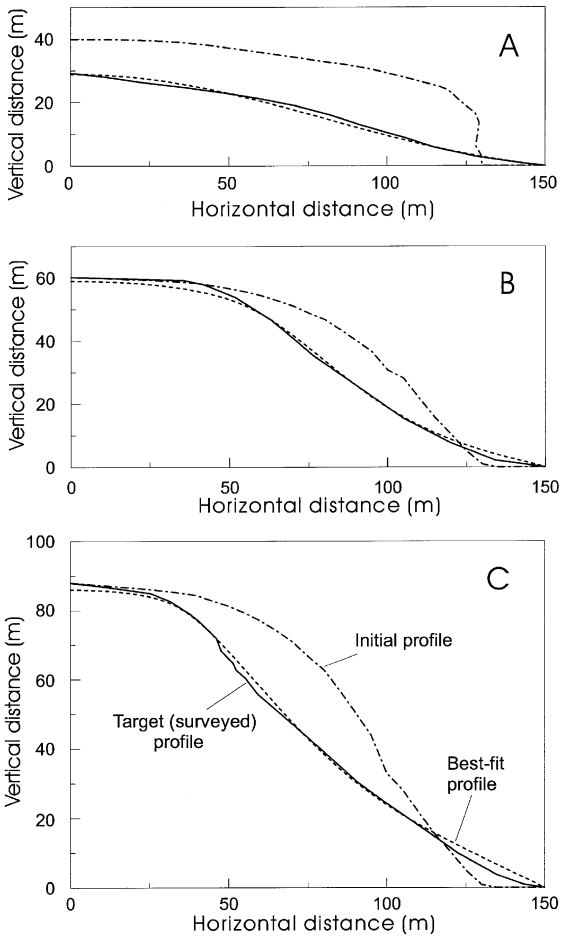

Fig. 9. Initial profile, modern profile, and best-fit profile produced by modeling for the three abandoned meanders along Cane Creek. For this modeling, all profiles were adjusted to the same horizontal length of 150 m. The following rates were used for the simulations: creep/solifluction rate (K) = 4 m^2 ka^{-1}, distance (m) at which wash becomes greater than creep (u) = 100 m, solution rate (r_s) = 30 mm ka^{-1}, rate of free degradation above threshold (α) = 0.8 mm year^{-1}, landslide threshold angle (g_ϕ) = 23°, talus angle (g_t) = 35°, and landslide travel distance = 60 m. (A) Highest cutoff meander (profile A1b). The mean absolute difference between the best-fit model profile and the actual profile is 0.69 m and the model age is 254 ka. (B) Intermediate cutoff meander (profile A2a). The mean absolute difference between the best-fit model profile and the actual profile is 1.04 m and the model age is 22 ka. (C) Lowest cutoff meander (profile A3b). The mean absolute difference between the best-fit model profile and the actual profile is 1.16 m and the model age is 33 ka.

ously, the age of the highest cutoff profile would be 717 ka (vs. a model age of 254 ka), that of the intermediate profile would be 233 ka (vs. 22 ka), and that of the lowest profile would be 50 ka (vs. 33 ka). Although the two age estimates for the lowest profile are in rough agreement, for profiles A1b and A2a the model ages are much younger than the ages estimated from the incision rate. This disparity may indicate that the assumed incision rate is too low or that excessively high process rates have been used in the model. One attempt to address this problem can be made by changing the parameter values in order to produce a model age nearly the same as the incision-rate age and then evaluating the plausibility of the new values. For the A1b profile, increasing u or decreasing α increases the age of the profile only slightly. A decrease in both creep rate and solution rate are required to produce the right age; neither alone is sufficient unless unrealistically low values are used. For example, a creep rate of 1.5 m^2 ka^{-1} and a solution rate of 10 mm ka^{-1} give a model age of 706 ka, close to the 717 ka age derived from the assumed incision rate. For the A2a profile, the required values are still lower. To produce a model age of 230 ka, for example, creep must be reduced to 0.7 m^2 ka^{-1}, solution to 7 mm ka^{-1}, and rate of free degradation above threshold to 0.1 mm year^{-1}. These values seem improbably low to us, suggesting that the valley incision rate is higher than the assumed 60 m ka^{-1}.

Another disparity concerns the two younger profiles. According to their elevations AML (14 vs. 3 m), the intermediate hillslope profile A2a should be more than four times as old as the lowest profile A3b. In contrast, modeling shows that A3b is older than A2a (Figs. 8 and 9). This discrepancy might be explained as follows. First, an age difference of 1.5 times, given the uncertainties of modeling, essentially means that the two profiles do not differ in age. Such similarity in age might stem from the stratigraphy. Fig. 6 shows that the base of both slopes (i.e., the floor of the abandoned meander) is in the Chattanooga Shale, despite the fact that site A2 is higher above the present stream than is A3. Downcutting after meander abandonment thus may have occurred rapidly in both cases, at a rate much higher than the long-term incision rate of the valley, with factors other than time determining the depth of post-abandonment incision. For example, a transition of the valley bottom from cherty limestone into the under-

lying shale might have produced a lowering of the valley gradient, accomplished by greater incision upstream (where cutoff A2 is located) than downstream (where cutoff A3 is located).

As a check on the dependence of modeling results on the peculiarities of individual profiles, a second profile at each of the three Cane Creek cutoffs was modeled using the same process rates and initial profiles as used for the first profile. For A3c, the age was 17 ka (vs. 33 ka for A3b); for A2b the age was 15 ka (vs. 22 ka for A2a); and for A1c the age was 358 ka (vs. 254 ka for A1b). Thus, the ages are at least within a factor of two and usually somewhat closer than that.

The talus thicknesses indicated by seismic refraction are compatible with the modeling results for the younger two profiles, but not for the oldest where most of the talus deposited earlier in the slope evolution is subsequently removed by erosion. A possible explanation for this discrepancy is that seismic velocity interpreted as talus here is, in fact, residuum.

A model detail of interest is the amount of material retained in the most-downslope cell. Presuming that the hillslope declines passively after abandonment of the meander, a large amount of hillslope debris would be expected to accumulate at the base of the slope. In fact, however, retaining even several percent of the flux into the basal cell produces a profile that, because of the prominence of its footslope, matches the actual profile much more poorly than when the cell is set to retain none of the flux into it. (Retaining large percentages generally leads to model instability.) Therefore, all of the simulations reported here retained no sediment in the basal cell. We are uncertain whether this result simply reflects limitations of the model, or whether geological explanations are involved. Perhaps the solution rate for fragmental hillslope debris is somewhat greater than the rate for intact bedrock. Another partial explanation may involve the process of meander abandonment. Rather than being a simple on–off switch, abandonment was probably a gradual process, with a progressive reduction in the frequency and size of flows through the meander loop while the cut-off course was being established. Even though the decreasing flows may not have been sufficient to undermine the hillslope, they may still have been capable of removing part of the debris shed by the declining slope.

6. Conclusions

The study of hillslope profiles on the outside walls of abandoned bedrock meanders appears to be a useful means of studying hillslope evolution. Maximum slope angles on the undercut slopes of the abandoned meander, as measured on contour maps, decline as a function of height AML. For more detailed comparisons involving surveys of slope profiles, the compared meanders should occur along a short reach of the same stream, as is the case for the Cane Creek sites. Comparisons of hillslope profiles associated with cutoff meanders at various heights AML show that the free or cliff face disappears soon after the abandonment occurs, as the profiles associated with even the lowest cutoff meanders show no or only a small free face. Profiles associated with cutoffs up to about 20 m AML maintain straight segments with angles ranging from 34° to 38°; average slope angles decrease, however, as the straight segment becomes shorter. The oldest slopes, those on meanders 30 m or greater AML, have developed into convex–concave slopes with maximum slope angles of 15°.

Modeling hillslope evolution is particularly useful in this setting. If the valley incision rate is known, an age can be estimated for the cutoff and hence for the hillslope. Alternatively, if hillslope process rates are known, a model age obtained for the hillslope can be used to estimate an incision rate. Even where both incision rates and hillslope process rates are poorly constrained, as in the present setting, modeling allows assumptions about specific rates to be evaluated by determining their implications for other rates.

The application of a hillslope evolution model allows several insights that otherwise might not have been possible. First, experimentation with heights of initial profiles using best-fit criteria suggests that since abandonment of the highest cutoff, plateau lowering has been one-fourth the rate of valley incision, a result compatible with the ratio of previously measured chemical denudation rates on the Tennessee Highland Rim and Central Basin. In contrast,

for the two lower cutoffs, the assumption producing the best modeling results is that the plateau did not lower at all after the abandonment of these cutoffs. This finding is compatible with other modeling results discussed below.

Once the initial profiles had been derived, further experimentation allowed selection of model parameter values that provide optimum fits of model profiles to the target profiles. The ages of two of the model profiles were found to be much less than what would be predicted from the estimated incision rate of 60 m Ma^{-1}. Reducing the model parameter values sufficiently to produce a model profile age similar to that predicted from the valley incision rate, however, requires that improbably low rate values be assigned, suggesting that the estimated incision rate is too low. In addition, the model age of the intermediate profile was found to be younger than that of the lowest hillslope, whereas based on relative heights AML (14 vs. 3 m), the intermediate profile should be more than four times as old. This finding can be explained by the assumption that valley incision was much faster after abandonment of the two lower meanders than it had been previously, so that the plateau surface indeed was lowered very little during this final phase of valley downcutting, as suggested above. This hypothesis is supported by the position of the floors of the two lowest meanders in the soft rocks just below the resistant Fort Payne Formation, making rapid subsequent valley incision probable.

Modeling a second set of profiles from each of the three abandoned meanders on Cane Creek produces profile ages roughly similar to those obtained from the first set, demonstrating that model ages are not greatly affected by small differences in target profiles.

A final insight concerns the process rates that need to be determined in order to allow more precise modeling of hillslopes. For young hillslopes, the rate of free degradation above threshold is by far the most important; creep, wash, and solution rates have much less effect on slope evolution. On the other hand, for old hillslopes, the rate of free degradation above threshold is not very important, but the rates of creep, wash, and solution become critical. Determination of modern rates alone, however, is not sufficient, as the hillslopes very likely have been affected by periglacial climates of the Pleistocene.

Acknowledgements

We wish to thank the dozens of students who participated over the years in the field work for this study. Students who made particularly large contributions include Frank Bogle and Anthony Crist (surveying) and Mario Casteneda (seismic work).

References

Andrews, D.J., Bucknam, R.C., 1987. Fitting degradation of shoreline scarps by a nonlinear diffusion model. J. Geophys. Res. 92, 12857–12867.

Andrews, D.J., Hanks, T.C., 1985. Scarp degraded by linear diffusion: inverse solution for age. J. Geophys. Res. 90, 10193–10208.

Carson, M.A., Kirkby, M.J., 1972. Hillslope Form and Process. Cambridge Univ. Press, London, UK, 475 pp.

Colman, S.M., Watson, K., 1983. Ages estimated from a diffusion equation model for scarp degradation. Science 221, 263–265.

Culling, W.E.H., 1960. Analytical theory of erosion. J. Geol. 68, 336–344.

Delcourt, H.R., 1979. Late-Quaternary vegetation history of the Eastern Highland Rim and adjacent Cumberland Plateau of Tennessee. Ecol. Monogr. 49, 255–280.

Froelich, A.J., Hoffman, M.F., Taunton, S.S., 1992. Preliminary Results of Coring Surficial Deposits in the Winchester 30×60 Minute Quadrangle, West Virginia and Virginia. U.S. Geol. Survey Open-File Report 92-395, 16 pp.

Hanks, T.C., Schwarz, D.P., 1987. Morphological dating of the pre-1983 fault scarp on the Lost River fault at Doublespring Pass road, Custer County, Idaho. Bull. Seismol. Soc. Am. 77, 837–846.

Hanks, T.C., Wallace, R.E., 1985. Morphological analysis of the Lake Lohonton shoreline and Beachfront fault scarps, Pershing County, Nevada. Bull. Seismol. Soc. Am. 835–846.

Hanks, T.C., Bucknam, R.C., Lajoie, K.R., Wallace, R.E., 1984. Modification of wave-cut and faulting-controlled landforms. J. Geophys. Res. 89, 5771–5790.

Hooper, D.M., 1995. Computer-simulation models of scoria cone degradation in the Colima and Michoac án-Guanajuato volcanic fields, Mexico. Geofis. Int. 34, 321–340.

Hooper, D.M., 1998. Computer-simulation models of scoria cone degradation. J. Volcanol. Geotherm. Res. 83, 241–267.

King, L.C., 1953. Canons of landscape evolution. Geol. Soc. Am. Bull. 64, 721–752.

Kirkby, M.J., 1971. Hillslope process-response models based on the continuity equation. In: Brunsden, D. (Ed.), Slopes: Form and Process. Institute of British Geographers Special Publication 3, London, pp. 15–30.

Kirkby, M.J., 1973. Landslides and weathering rates. Geol. Appl. Idrogeol., Bari 8, 171–183.

Kirkby, M.J., 1984. Modelling cliff development in South Wales: savigear reviewed. Z. Geomorphol. 28, 405–426.

Kirkby, M.J., 1987. General models of long-term slope evolution

through mass movement. In: Anderson, M.G., Richards, K.S. (Eds.), Slope Stability. Wiley, London, pp. 359–379.

Kirkby, M.J., 1992. An erosion-limited hillslope erosion model. In: Schmidt, K.-H., de Ploey, J. (Eds.), Functional Geomorphology: Landform Analysis and Models. Catena Supplement 23, pp. 157–187.

Kirkby, M.J., Naden, P.S., Burt, T.P., Butcher, D.P., 1992. Computer Simulation in Physical Geography. Wiley, Chichester, UK, pp. 85–90.

Mayer, L., 1984. Dating Quaternary fault scarps formed in alluvium using morphological parameters. Quat. Res. 22, 300–313.

Mooney, H.M., 1984. Handbook of Engineering Geophysics, vol. 1, Seismic Bison Instruments, Minneapolis, MN, 204 pp.

Nash, D.B., 1980. Morphological dating of degraded normal fault scarps. J. Geol. 88, 353–360.

Nash, D.B., 1984. Morphological dating of fluvial terrace scarps and fault scarps near West Yellowstone, Montana. Geol. Soc. Am. Bull. 95, 1413–1424.

Paine, A.D.M., 1985. "Ergodic" reasoning in geomorphology: time for a review of the term? Prog. Phys. Geogr. 9, 1–15.

Pierce, K.L., Colman, S.M., 1986. Effect of height and orientation (microclimate) on geomorphic degradation rates and processes, late-glacial terrace scarps in central Idaho. Geol. Soc. Am. Bull. 97, 869–885.

Reesman, A.L., Godfrey, A.E., 1981. Development of the Central Basin of Tennessee by chemical denudation. Z. Geomorphol. 25, 437–456.

Rich, J.L., 1914. Certain types of stream valleys and their meaning. J. Geol. 22, 469–497.

Rosenbloom, N.A., Anderson, R.S., 1994. Hillslope and channel evolution in a marine terraced landscape, Santa Cruz, CA. J. Geophys. Res. 99, 14013–14029.

Sasowsky, I.D., White, W.B., Schmidt, V.A., 1995. Determination of stream-incision rate in the Appalachian plateaus by using cave-sediment magnetostratigraphy. Geology 23, 415–418.

Savigear, R., 1952. Some observations on slope development in South Wales. Inst. Brit. Geogr. Trans. 18, 31–51.

Skempton, A.W., 1964. The long-term stability of clay slopes. Geotechnique 2, 75–102.

Wilson, C.W., Jr., Marcher, M.V., 1968. Geologic map and mineral resources summary of the Burgess Falls quadrangle, Tennessee. State of Tennessee Division of Geology, GM 326-SE and MRS 326-SE.

Wood, A., 1942. The development of hillside slopes. Geol. Assoc. Proc. 53, 128–138.

Young, A., 1972. Slopes. Longman, London, 288 pp.